Casimir forces of metallic microstructures into cavities

George Kenanakis, Costas M. Soukoulis, and Eleftherios N. Economou

Phys. Rev. B **92**, 075430 — Published 19 August 2015

DOI: 10.1103/PhysRevB.92.075430

Casimir forces of metallic micro-structures into cavities

George Kenanakis,[1,*] Costas M. Soukoulis,[1,2] and Eleftherios N. Economou[1]

[1] *Institute of Electronic Structure and Laser, Foundation for Research & Technology-Hellas, N. Plastira 100, 70013, Heraklion, Crete, Greece*

[2] *Ames Laboratory-USDOE, and Department of Physics and Astronomy, Iowa State University, Ames, 50011 Iowa*

*gkenanak@iesl.forth.gr

A novel theoretical estimate of the Casimir force of a metallic structure embedded into a cubic cavity is proposed. We demonstrate that by calculating the eigenmodes of the system we can determine the Casimir force which can be either attractive or repulsive by simply changing the geometry of the structures relative to the walls of the cavity. In this analysis, several cases of structures are taken into account from rectangular slabs to chiral "omega" particles, and the predicted data are consistent with recent literature. We demonstrate that the side walls of the studied cavity contribute decisively to the repulsive Casimir force between the system and the nearby top surface of the cavity. Finally, we have provided evidence that the medium embedded into the studied cavity (and especially its permittivity) can change the intensity of the Casimir force, while its repulsive nature once established (thanks to favorable geometrical features) remain quite robust.

PACS number(s): 42.50.Ct, 12.20.-m, 78.20.Ek, 81.05.Xj.

I. INTRODUCTION

The Casimir force has been widely studied over the past years [1-4], giving emphasis to its practical applications [5-6]. According to H.B.G. Casimir, who discovered this force [7], two neutral perfectly conducting parallel surfaces in vacuum separated by a distance d attract each other by a force F due to the quantum fluctuations of the vacuum field [7-8]: $(F/A) = -\frac{\pi^2}{240}\frac{\hbar c}{d^4}$, where $\hbar$ (h-bar) is the Planck constant divided by 2π, and A is the area. The Casimir force becomes more pronounced if the dimension goes to nanoscale, leading to stiction and adhesion on the surface [2] which is a challenge for flexibly operating the micro/nano-electro-mechanical system devices (MEMs).

Lifshitz's extended theory [9] generalized the calculation of Casimir force between two parallel plates, 1 and 2, characterized by frequency-dependent dielectric functions $\varepsilon_1(\omega)$ and $\varepsilon_2(\omega)$. The formula for the force or the interaction energy per unit area can be expressed in terms of the reflection amplitudes r_j^{ab} (j=1, 2) [10] at the interface between the vacuum and the plate j, giving the ratio of the reflected electromagnetic wave of polarization a over the incoming wave of polarization b. Each a and b stands for either TM (or p) or TE (or s) polarized waves. The frequency integration is performed along the imaginary axis by setting $\omega=i\xi$. The interaction energy per unit area is given by:

$$\frac{E(d)}{A} = \frac{\hbar}{2\pi}\int_0^{+\infty} d\xi \int \frac{d^2k_{\parallel}}{(2\pi)^2} \ln\det G\,; \qquad R_j = \begin{vmatrix} r_j^{ss} & r_j^{sp} \\ r_j^{ps} & r_j^{pp} \end{vmatrix} \qquad (1)$$

where $G = I - R_1 \cdot R_2 e^{-2K_0 d}$, I is the unit matrix and $K_0 = \sqrt{k_{\parallel}^2 + \varepsilon_0 \mu_0 \xi^2}$; ε_0 and μ_0 are the permittivity and permeability of free space, and d is the distance between the two parallel plates. A negative slope of $E(d)$ corresponds to a repulsive force, while a positive one corresponds to an attractive force.

The calculation of the Casimir force was extended to other than planar geometries [1,12,13], because a unique property of this force is its strong dependence on the geometry of the interacting media, switching from attractive to repulsive; this makes the Casimir effect a likely candidate for applications in nanotechnologies and MEMs [11]. The attractive Casimir forces predicted to exist between electrically neutral bodies [11], while repulsive forces are predicted to exist inside of an empty sphere [1] and an empty rectangular cavity [12-13] with perfectly conducting walls.

In this manuscript we study numerically the effect of the geometry of a metallic structure inside a metallic cavity on the attractive or repulsive character of the Casimir force. More explicitly, we introduce several metallic structures of various sizes and shapes inside a 3×3×3 μm^3 metallic cavity and close to the top surface; then the basic approach employed is the calculation of the eigenmodes of the system in terms of which we determine the Casimir interaction and hence the force which can be either attractive or repulsive by simply changing the geometrical features of the structures.

II. STRUCTURES UNDER INVESTIGATION

The structures employed in the present study, shown in Fig. 1 (a-d), were placed inside a 3×3×3 μm^3 metallic cavity, close to its top surface [see Fig. 1(a)]; their geometrical parameters are detailed in the caption of Fig. 1.

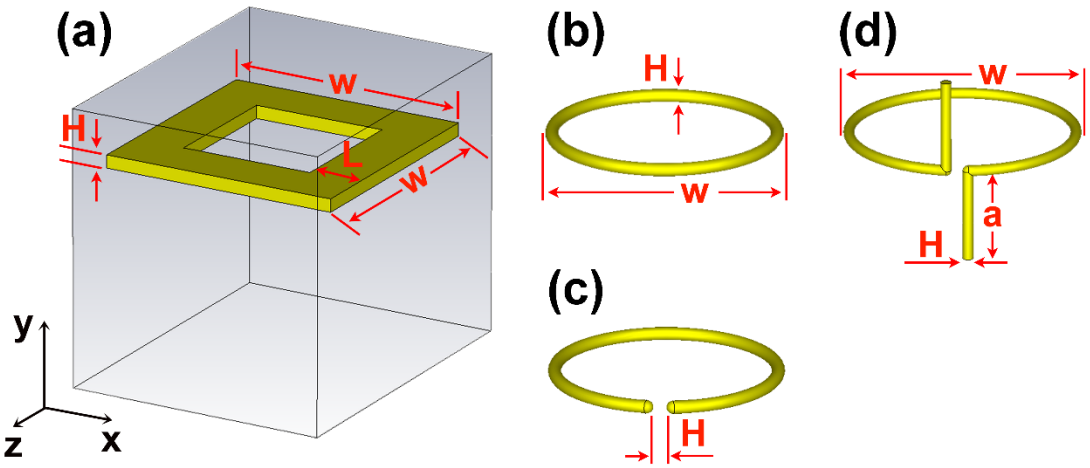

FIG. 1. (Color online) Schematic of the structures under investigation; w = 2.75 μm, H = 0.15 μm, L = 0.055-1.375 μm, and a=0-1.125 μm, respectively. In Fig. 1(a) one can notice the 3×3×3 μm^3 metallic cavity, in which each of the studied structures are embedded in, close to its top surface.

As one can see in Fig. 1, apart from the square structures of Fig. 1(a) with L = 0.055-1.375 μm, three more structures embedded in metal cavities were studied [see Figs. 1(b), 1(c) and 1(d) for details]; a metallic ring of circular cross-section with diameter H=0.150 μm and outer diameter of w=2.75 μm [Fig. 1(b)], a Split Ring Resonator (SRR) -like structure (loop) having the same geometrical dimensions as the ring in Fig. 1(b) and a gap of H=0.150 μm [Fig. 1(c)], and a chiral "omega" structure consisting of an open circular loop with exactly the same dimensions like the SRR structure of Fig. 1(c) and two short wires with a length a=1.0 μm, as seen in Fig. 1(d).

III. NUMERICAL SIMULATIONS, ESTIMATION OF THE CASIMIR FORCE

For the numerical simulations we used the Eigenmode solver of a commercial three-dimensional full-wave solver (CST Microwave Studio, Computer Simulation Technology GmbH, Darmstadt, Germany) based on the Finite Integration Technique. For each design we considered a single (3×3×3, μm^3) calculation boundary box under vacuum, as shown in Fig. 1(a), with the tangential electric field being zero (E_t=0) along *x*, *y* and *z* directions, acting like a perfectly metallic cavity, while all the metallic structures (yellow color in Fig. 1) were treated as perfect electric conductors (PEC), since the Eigenmode solver of the software mentioned above does not support lossy and/or dispersive metal materials.

At this point it should be noted that Casimir force arises from the fluctuations of the electromagnetic field mainly in the region between the metallic surface (a), and from a van der Waals type of interaction due to electrostatic mutual polarization of the metallic materials (b). The (a) part can equivalently be incorporated into (b) by including retardation effects [14]. The first contribution dominates at distances much larger than a characteristic absorption length $\lambda_0 \equiv c/\omega_0$ [14], where ω_0 is a frequency corresponding to a characteristic excitation energy $\hbar\omega_0$ in a metal, such as a plasma energy. The length λ_0 physically is the one beyond which the usual electrostatic van der Waals interaction has to be corrected as to incorporate retardation effects [14]. The second contribution to the Casimir force mentioned above, prevails at much smaller distances [14], typically for λ_0 in the order of 30 nm [15]. As a result, our calculations, although we consider PEC structures and not realistic frequency dependent permittivity of the metallic structures and the walls of the cavity, are safe.

Moreover, as in our case, there are several research groups [16-17] calculating Casimir force considering PEC structures into metallic cavities with PEC walls filled with non-dispersive media, indicating that the effect of loss and dispersion is quite mild and that the results obtained using the PEC assumption describe well the physics of the system.

The structures under investigation were placed into the cavity described above, initially at a distance *d* of 100 nm from its top surface (check Fig. 2 for the case of the structure presented in Fig. 1(a) with *L*=150 nm). Using the Eigenmode solver of CST software the first 500 Eigenmodes of the system (PEC structure into the cavity) were calculated. The energy of the system was calculated using the formula [11]:

$$E_d = \frac{1}{2}\sum_{i=1}^{500} \hbar \cdot \omega_i \qquad (2),$$

where *d* denotes the distance between the center of the studied structure and the top surface of the cavity, and ω_i denotes each of the 500 calculated Eigenmodes. Then, each of the PEC structures was moved along *y*- axis at a distance of 200 nm and 500 nm from the top surface of the boundary box respectively [see Fig. 1(a)], and the corresponding energies E_{200nm} and E_{500nm} were calculated.

In order to estimate the Casimir force (F) along *y*- axis at a distance *d*=300 nm between the top surface of the cavity and the PEC structure, the following formula was used:

$$F_{y,300nm} = \frac{E_{d=500nm} - E_{d=100nm}}{500nm - 100nm} \approx \frac{E_{d=200nm} - E_{d=100nm}}{200nm - 100nm} \qquad (3),$$

where $E_{d=500nm}$, $E_{d=200nm}$, and $E_{d=100nm}$ are the calculated energies at distances of 500 nm, 200 nm, and 100 nm, respectively.

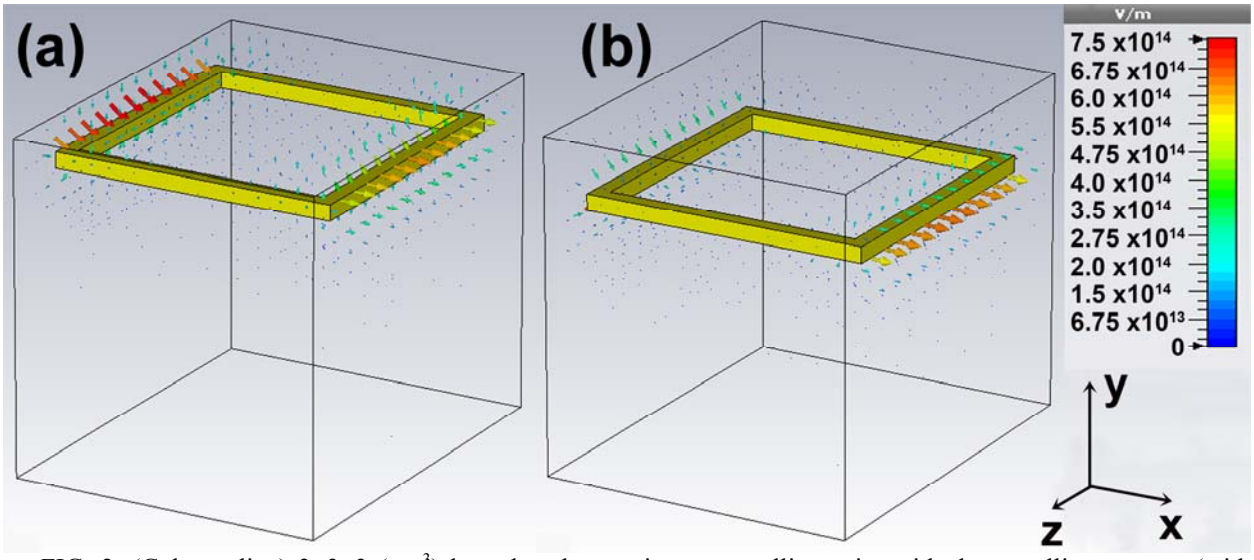

FIG. 2. (Color online) 3×3×3 (μm^3) boundary box acting as metallic cavity with the metallic structure (with L=0.150μm) embedded into it. The distance of the structure from the top surface of the boundary box is 100 nm (a), and 500 nm (b), respectively. A snapshot of the electric field distribution on the metallic structure embedded into the 3×3×3 (μm^3) boundary box is shown.

As one can notice from Fig. 2, the contribution of the side walls of the metallic cavity is more intense than the one from the top (and of course the bottom) walls. Following the methodology described above, we have calculated the Casimir force of the structures presented in Fig. 1(a) for several values of L, keeping H constant and equal to 150 nm. We have repeated these calculations for H=50 nm and for H=300 nm, changing the geometry of Fig 1(a) from a rectangular loop with L=0.055 μm (L/H=0.367) to a square plate with L=1.375 μm (L/H=9.167). In Fig. 3 we present the Casimir force of the proposed structure of Fig. 1(a) along y- axis, as a function of the ratio L/H.

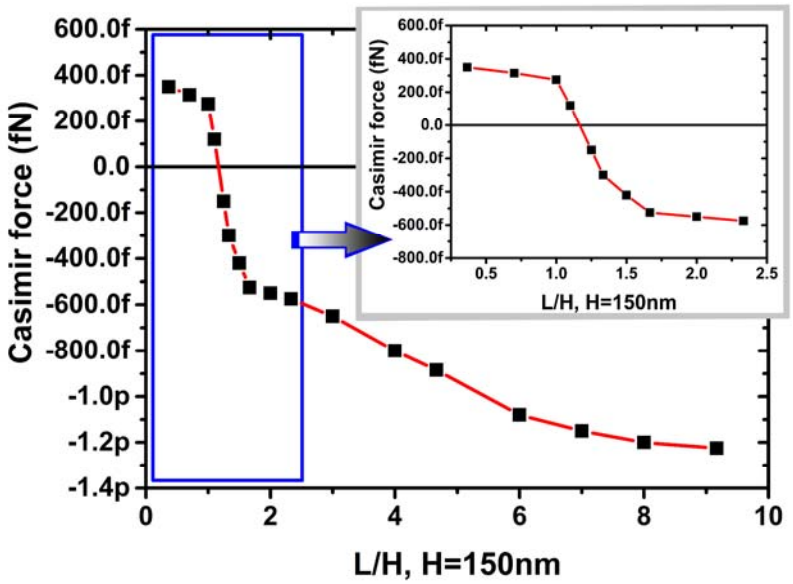

FIG. 3. (Color online) Casimir force along y- axis at a distance d=300 nm between the top surface of the cavity and the proposed structure of Fig. 1(a) as a function of the ratio L/H. In the inset of Fig. 3 one can see a more detailed presentation of the Casimir force for L/H=0.25-2.5.

As seen from Fig. 3, there is a certain value of the ratio L/H=1.167 where the Casimir force along y-axis (at a distance of about $d \approx 225$ nm between the top surface of the cavity and the PEC structure) equals to zero. Moreover, for $1.167<L/H\leq 9.167$ negative Casimir force is obtained, indicating that the force is attractive, while for $1.167>L/H\geq 0.3667$ positive Casimir force is achieved, demonstrating that the force is repulsive.

At this point it is worth mentioning again that further numerical simulations have been performed (not shown here), for values of H other than 150 nm: H=50 nm and H=300 nm, respectively and changing the values of L. As in the case of H=150nm and L=0.055-1.375 μm (L/H=0.367-9.167), we found again using these other values of H that there is a region for L/H in which negative (attractive) Casimir force is obtained, while for a different region of L/H positive (repulsive) Casimir force is achieved and that the transition occurs for the same value of the ratio L/H. Thus, it was concluded that it is the ratio L/H which controls the sign of the Casimir force between the object and the top wall in the presence of side walls. This behavior is attributed to a competition between the interaction with the side walls, which is producing a repulsive force along the y-direction, and the interaction with the top wall, which produces an attractive force along the same direction. (The bottom wall is too far away to play any role). Obviously as L is increasing, the interaction with the top is enhanced and overcomes the repulsion. On the other hand, as the length H is increasing, the side walls-due repulsion is strengthened and wins over the attraction. Thus, it is the ratio L/H which controls the sign of the Casimir force between the object and the top wall in the presence of side walls. We think, on the basis of our results and those of Ambjørn and Wolfram [13], that in general the presence of a kind of surrounding side metals contribute a repulsive component to the Casimir force.

Let us summarize the preceding arguments: Our assertion that the side walls contribute a repulsive component to the force along the y-direction, while the top wall an attractive one, is supported both by the obtained field distributions (Figs. 2 and 4) and the simulations showing that (attractive component)/(repulsive component) is a monotonically decreasing function of the ratio L/H.

According to Zhao *et al.* [18] the intensity of the repulsive Casimir force can be optimized by increasing the inductance of the structures. Indeed, the rectangular and the circular metallic rings of Fig. 1(a) with L/H=1 and Fig. 1(b) respectively give almost the same repulsive Casimir forces; 275 fN and 273.7 fN, respectively. When a gap is created into the metallic ring structure [see Fig. 1(c)] (and thus inductance is induced), the Casimir force is remaining repulsive, while its intensity is raised to 283.5 fN.

Another important parameter for enhancing the repulsive Casimir force is the chiral properties of the structures [18-19]. As already stated [15,18], chiral metamaterials (CMMs) are candidates to realize the repulsive Casimir force, while the existence of a repulsive Casimir force depends upon the strength of the chirality. Indeed, the so-called “omega” particle [18,20] defined in Fig. 1(d) provided a repulsive Casimir force along y- axis with an intensity of ~ 315.1 fN, enhanced by ~11.2 % compared to the SRR structure presented in Fig. 1(c), exhibiting the highest repulsive Casimir force compared to all the structures studied in this work (see Figs. 1 for reference).

Moreover, as already stated for the structures shown in Fig. 2, the contribution of the side walls of the metallic cavity is more intense than the one from the top wall (the interaction with the bottom wall is still quite small even in the case of omega particle shown in Fig.4, where the distance between the lower edge and the bottom is 0.75 μm). This is confirmed by the electric field distribution shown Fig. 4, where the upper edge of the “omega” particle is at a distance of 100 nm from the top surface of the cavity [the distance between the loop of the “omega” structure and the top surface of the cavity equals to 1.1 μm (0.1 μm + a), and the distance of the lower edge from the bottom surface is 0.75 μm (3 - 2a - 0.15 μm - 0.1 μm), where a is the length of the “omega’s” wires, taken to be equal to 1.0 μm, in Fig. 4].

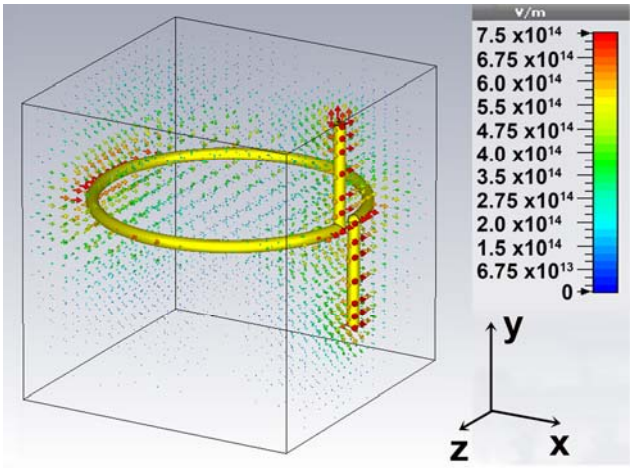

FIG. 4. (Color online) Electric field distribution on the "omega" particle embedded into the 3×3×3 (μm^3) cavity at a distance of 100 nm between the upper edge of the wire and the top surface.

The "omega" particle can be considered as a connection of two small wire antennas: a short electric dipole antenna of length *2a* and a small loop antenna with radius 2.75/2 μm [21-23]. Since the length (*a*, in Fig. 5) of the wires of the "omega" particle enhances the chirality the structure, its effect on the Casimir force was further investigated. In Fig. 5 one can see the intensity of the Casimir force along *y*-axis (in fN) of the proposed "omega" particle embedded into a 3×3×3 (μm^3) cavity, as a function of its wire's length, *a*. For this type of calculations, the loop of the "omega" particle was placed at a symmetric position in the 3×3×3 (μm^3) cavity, and several cases of wires were studied with length *a*=0.0-1.125 μm. Then, the "omega" particle was moved towards the top surface of the cavity by 100 nm and 500 nm, and the Casimir force was calculated using the formulas (2) and (3) mentioned above.

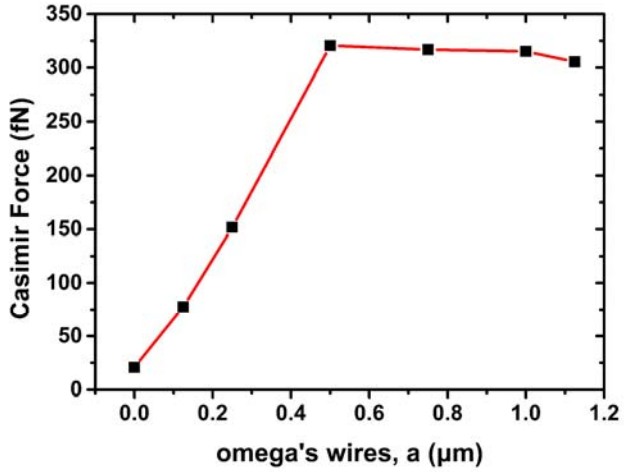

FIG. 5. (Color online) Repulsive Casimir force of the proposed "omega" particle embedded into a 3×3×3 (μm^3) cavity, as a function of its wire's length, *a*. For this type of calculations, as opposed to the one shown in Fig.4, the loop of the "omega" particle was placed at a symmetric position in the 3×3×3 (μm^3) cavity, and several cases of wires were studied with length a=0.0-1.125 μm.

As expected, the shortening of the wires of the "omega" particle produces a less chiral structure [21], and thus the Casimir force is minimized (check Fig. 5). Moreover, as one can notice from Fig. 5, for *a*=0.5 μm, the repulsive Casimir force becomes maximum reaching a value of 320.5 fN, while for wires' length $0.5 \leq a \leq 1.125$ μm the Casimir force almost saturates, being from 320.5 fN to 305.48 fN, respectively. The minor drop observed beyond *a*=1 μm is due to the increased interaction with the bottom surface as a result of which a force pointing along the positive y-axis appears.

In order to verify the effect of the side walls of the cavity studied in this work, a new cavity (boundary box) was designed with dimensions of 30×30×30 μm^3 (E_t=0 along *x*-, *y*- and *z*- directions). A single "omega" particle (with dimensions as described in Fig. 5) was placed inside the 30×30×30 μm^3 cavity at a distance of 100 nm between its upper edge and the top surface. The "omega" particle was displaced along *y*- axis (see Fig. 2) at a distance of 500 nm from the top surface of the cavity, and the Casimir force was calculated using the formulas (2) and (3) mentioned above, being practically zero (~7.7×10^{-5} fN). Indeed, the Casimir force is 6 orders of magnitude less than the one calculated for the 3×3×3 (μm^3) cavity (315.1 fN), reaching the limits of the computational method proposed within this work. This conclusion is also confirmed by the electric field distribution which shows that less intensities are recorded (not shown here).

At this point it should be noted that the Casimir force along *x*- and *z*- axes were also calculated, following the procedure described above, by moving the proposed PEC structures inside the 3×3×3 μm^3 cavity along *x*- and *z*- direction, respectively [see Fig. 1(a)], and applying similar equations to (2) and (3). For instance, the Casimir Force of the "omega" particle presented in Fig. 1(d) and Fig. 4 along *x*- axis is remaining repulsive, upon moving the "omega" particle along *x*- axis, from 20 nm to 100 nm from the right side wall (see Fig. 4), with an intensity of $F_{x,60nm}$ ~16.84 fN, while the movement of the "omega" particle along *x*- axis, towards the left side wall (see Fig. 4), provides a similar repulsive Casimir force, with an intensity of $F'_{x,60nm}$ ~12.28 fN. Finally, the relocation of the "omega" particle along *z*- axis, from 20 nm to 100 nm from the back (or front) side wall (see Fig. 4), produces a repulsive Casimir force along *z*- axis being $F_{z,60nm}$ ~12.14 fN (or $F'_{z,60nm}$ ~11.82 fN). It is more than clear that the Casimir force of the "omega" particle of Fig. 1(d) embedded into the 3×3×3 μm^3 cavity along *x*- and *z*- axis is always repulsive and almost constant to 11.82-16.84 fN, no matter of the movement of the particle along *x*- or *z*- direction. Due to the symmetry of the "omega" particle, its movement along *z*- axis, either towards the front or the back side wall (see Fig. 4), does not produce different Casimir forces; $F_{z,60nm}$ ~12.14 fN (or $F'_{z,60nm}$ ~11.82 fN). On the other hand, the "omega" particle is not symmetric along the *y*-*z*- plane, and thus one may expect a different Casimir force when displacing the particle along *x*- axis towards the left or right side wall (see Fig. 4). Indeed, when the small wire antennas of the "omega" particle (which induce chirality to the structure) are closer to the right side wall, a more intense Casimir force is recorded $F_{x,60nm}$ ~14.84 fN. Thus, we conclude that the Casimir force deployed between the "omega" particle and the 3×3×3 μm^3 metallic cavity is more sensitive and intense along *y*- axis than the other directions (see Fig. 4). Moreover, under the geometrical parameters remaining within proper range of values, the Casimir Force is repulsive.

In order to fully study the Casimir force of the proposed structures enclosed into the 3×3×3 μm^3 cavity, the medium of the cavity was assumed to be a liquid dielectric the permittivity of which changed from that of the vacuum to that of the water [24-26]. According to several research groups [24-26], the medium in which the metal structures are embedded in plays a significant role in the nature of the reported Casimir force (attractive or repulsive). Thus, we have investigated further the PEC "omega" particle presented in Fig. 1(d), studying the effect of several media (with various, ε, and permeability values, μ, respectively) into the 3×3×3 (μm^3) cavity on the Casimir force between the top surface of the cavity and the structure.

As already stated, the results presented in Figs. 3 and 5 refer to PEC structures placed into the 3×3×3 (μm^3) metallic cavities under vacuum (with ε=1 and μ=1). In Fig. 6 we present Casimir force for the "omega" particle presented in Fig. 1(d) embedded into the 3×3×3 (μm^3) cavity filled with different dielectric liquids with several ε values varying from 1 (vacuum) to 78 (water), and μ=1.

It is worth mentioning that as we increase the permittivity ε of the liquids within the cavity, from 1 to 78 (keeping the permeability μ constant equal to 1), the Casimir force on the omega-particle remains

repulsive, while its intensity decreases from 315.1 fN (case of vacuum) to 6.14 fN (case of water; ε=78, μ=1). As it was shown in reference [14], the Casimir force is directly related with the van der Waals interaction incorporating retardation effects. The latter represent the fluctuation of the electromagnetic field. It follows that the Casimir force is due to retarded interactions between fluctuating charges developed on the walls of the cavity and those on the system. These fluctuating charges are screened very effectively by a dielectric constant intervening between the walls and the system. For two dipoles this screening is proportional to $1/\varepsilon^2$.

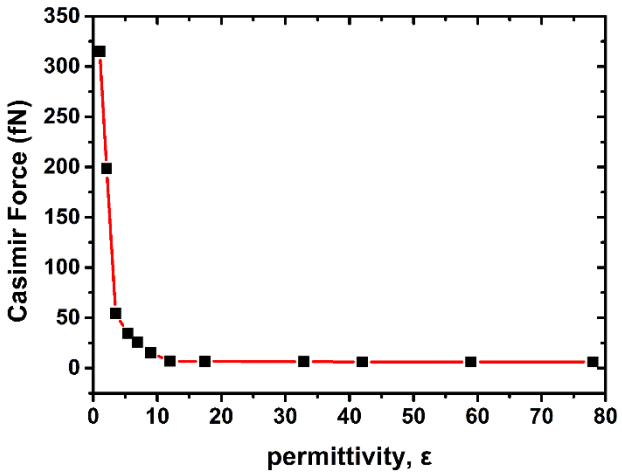

FIG. 6. (Color online) Repulsive Casimir force of the proposed "omega" particle embedded into a 3×3×3 (μm^3) cavity, filled with various media, as a function of their permittivity, ε.

On the other hand, if the cavities are filled with liquids with various values of μ from 1.7 to 4.02 (and ε being constant around ~32.7-34.82; case of methanol and nitrobenzene, respectively), the Casimir force is once more repulsive with an intensity of ~8.25 fN, indicating that the permeability of the liquids into the cavity is almost not affecting the Casimir force at all, in agreement with Lifshitz theory, where all magnetic properties of the involved media are neglected with the magnetic permeability set equal to 1 [27].

IV. CONCLUSIONS AND COMMENTS

In this work we have proposed a novel way of calculating the Casimir force of several metallic structures embedded in a cubic cavity by taking into account the Eigenmodes of the system. We have checked several designs (i.e. slabs, rings, loops and "omega" particles) and found out that repulsive Casimir force can be obtained by simply changing several geometrical features of the structures and mainly their distance from the side walls. We have also shown that the inductance and the chirality of the studied structures play a role. In addition, we have provided evidence that the medium embedded into the studied cavity (and especially its permittivity) can change the intensity of the Casimir force, while its repulsive nature once established (thanks to favorable geometrical features) remain quite robust. Finally, we want to comment on our limitation of assuming perfect metallic behavior as opposed to realistic frequency dependent permittivity of the metallic structures and the walls of the cavity. One can distinguish two physically distinct contributions to the Casimir force: One is due to the fluctuations of the

electromagnetic field mainly in the region between the metallic surfaces as envisioned originally by Casimir. The other is essentially a van der Waals type of interaction due to electrostatic mutual polarization of the metallic materials. It is well known [14] that the first contribution dominates at distances much larger than a characteristic absorption length $\lambda_0 \equiv c/\omega_0$ [14] and the second at distances much smaller than this length. Typical value for λ_0 is of the order of 30 nm [15]. Thus, since our calculations are for lengths considerably larger than this, we think that our conclusions are valid in spite of employing perfect metallic behavior.

ACKNOWLEDGMENTS

This work was supported by Greek GSRT project ERC02-EXEL, and by the European Research Council under ERC Advanced Grant No. 32081 (PHOTOMETA). Work at Ames Laboratory was partially supported by the Department of Energy (Basic Energy Sciences, Division of Materials Sciences and Engineering) under Contract No. DE-AC02-07CH11358 (computational studies).

REFERENCES

[1] T. H. Boyer, Phys. Rev. A **9**, 68 (1974).
[2] H. B. Chan, V. A. Aksyuk, R. N. Kleiman, D. J. Bishop, and F. Capasso, Sciense **291**, 1941 (2001).
[3] J. N. Munday, F. Capasso, and V. A. Parsegian, Nature **457**, 170 (2009).
[4] S. K. Lamoreaux, Phys. Rev. Lett. **78**, 5 (1997).
[5] F. M. Serry, D. Walliser, and J. Maclay, J. Appl. Phys. **84**, 2501 (1998).
[6] E. Buks and M. L. Roukes, Phys. Rev. B **63**, 033402 (2001).
[7] H. B. G. Casimir, Proc. Kon. Nederl. Akad. Wet. **51**, 793 (1948).
[8] E. M. Lifshitz and L. P. Pitaevskii, *Statistical Physics: Part 2* (Pergamon, Oxford, 1980).
[9] E. M. Lifshitz, Sov. Phys. JETP **2**, 73 (1956).
[10] A. Lambrecht, P. A. M. Neto, and S. Reynaud, New J. Phys. **8**, 243 (2006).
[11] M. Bordag, U. Mohideen, and V. M. Mostepanenko, Phys. Rep. **353**, 1 (2001).
[12] S. G. Mamaev and N. N. Trunov, Theor. Math. Phys. **38**, 228 (1979).
[13] J. Ambjørn and S. Wolfram, Ann. Phys. **147**, 1 (1983).
[14] A.A. Abrikosov, L.P. Gor'kov, I. Ye. Dzyaloshinskii, *Quantum Field Theoretical Methods in Statistical Physics, 2nd edn.* (Pergamon Press, Oxford, 1965).
[15] A. P. McCauley, R. Zhao, M. T. H. Reid, A. W. Rodriguez, J. Zhou, F. S. S. Rosa, J. D. Joannopoulos, D. A. R. Dalvit, C. M. Soukoulis, and S. G. Johnson, Phys. Rev. B **82**, 165108 (2010).
[16] T. A. Morgado, S. I. Maslovski, and M. G. Silveirinha, Opt. Express **21**, 14943 (2013).
[17] S. I. Maslovski and M. G. Silveirinha, Phys. Rev. A **82**, 022511 (2010).
[18] R. Zhao, T. Koschny, E. N. Economou, and C. M. Soukoulis, Phys. Rev. B **81**, 235126 (2010).
[19] R. Zhao, J. Zhou, T. Koschny, E. N. Economou, and C. M. Soukoulis, Phys. Rev. Lett. **103**, 103602 (2009).
[20] S. Tretyakov, A. Shivola, and L. Jylha, Photonics Nanostruct. Fundam. Appl. **3**, 107 (2005).
[21] D. L. Jaggard, A. R. Mickelson, and C. H. Papas, Appl. Phys. **18**, 211 (1979).
[22] Y. Ra'di and S. A. Tretyakov, New J. Phys. **15**, 053008 (2013).
[23] S. A. Tretyakov, F. Mariotte, C. R. Simovski, T. R. Kharina, and J.-P. Heliot, IEEE Trans. Antennas Propag. **44**, 1006 (1996).

[24] M. Bostrom, B. W. Ninham, I. Brevik, C. Persson, D. F. Parsons, and B. E. Sernelius, Appl. Phys. Lett. **100**, 253104 (2012).
[25] A. Milling, P. Mulvaney, and I. Larson, J. Colloid Interface Sci. **180**, 460 (1996).
[26] P. J. van Zwol and G. Palasantzas, Phys. Rev. A **81**, 062502 (2010).
[27] B. W. Ninham, and J. Daicic, Physical Review A **57**, 1870 (1998).